DOI: 10.1002/ejoc.200901150

Oligoaryl Cruciform Structures as Model Compounds for Coordination-Induced Single-Molecule Switches

Sergio Grunder,[a] Roman Huber,[b] Songmei Wu,[b] Christian Schönenberger,[b] Michel Calame,*[b] and Marcel Mayor*[a,c]

Dedicated to Giorgio Lazzarini

Keywords: Molecular electronics / Conducting materials / Arenes / Cross-coupling / Rearrangement

The synthesis of two new cruciform structures **3** and **4** comprising an oligo(phenylene-vinylene) (OPV) and a perpendicular oligoaryl bar – namely an oligophenylene (OP) (**3**) and a naphthyl–phenyl–naphthyl system (**4**) – is reported. The OPV rod consists of two terminal pyridine units, whereas the oligoaryl rod bears two terminal acetylsulfanyl groups as protected anchor groups. The OPV bar was assembled via a Horner–Wadsworth–Emmons reaction, which directly led to the desired *E,E* isomers. The perpendicular oligoaryl bars were assembled with a Suzuki reaction using the corresponding boronic acids, which were already fitted with an ethyl-trimethylsilane (ethyl-TMS) sulfanyl group. In a last step, the ethyl-TMS-protected sulfur atoms were transprotected to the thioacetyl units. The cruciform structures **3** and **4** are model compounds to investigate a coordination-induced single-molecule switch exploiting the potential-dependant different bonding strengths of the anchor groups to gold. Metal–molecule–metal junctions were formed using a mechanically controllable break junction (MCBJ) setup. Current traces of molecular junctions were statistically analyzed. Further investigations of model compounds consisting only of the single bar confirm that individual molecules carrying the required function for the switching experiments were trapped between two electrodes and were mainly immobilized via thiol–gold anchor bonds.

Introduction

The visionary concept of integrating designed molecular structures in electronic circuits as minute functional units is today called "molecular electronics" and roots in H. Kuhn's ideas of "molecular engineering" proposed in the 1960s.[1] Soon later, Aviram and Ratner discussed potential rectification emerging from a molecular structure based on a theoretical model.[2] While this pioneering suggestion moved molecules, as smallest unit providing the required structural variation, further into the focus of interest, the concept remained on a theoretical level due to the missing tools required to realize single-molecule transport experiments. Only within the last two decades the tremendous improvement of physical setups enabled the integration of monomolecular films,[3–8] small assemblies[9] and even single molecules providing an experimental base of "molecular electronics".[10–14] Electronic transport through single molecules was studied with various scanning probe setups ranging from designed molecular structures diluted in a matrix of a self-assembled monolayer (SAM)[15,16] to transient scanning probe break junctions.[17,18] Attempts to obtain more symmetric pairs of electrodes were based on mechanically controllable break junctions (MCBJ)[19–24] or electromigration techniques.[25–27] Numerous molecular structures have been integrated on a single-molecule level like alkanedithiols[28–32] as the commercially available working horse of physicists to more rigid structures like for instance oligo(phenylene-vinylenes) (OPVs),[33,34] oligo(phenylene-ethynylenes) (OPEs)[33,35–37] or oligophenylenes.[38] Rectification as first electronic function was demonstrated with suitably designed molecular structures in monomolecular films[3,4,39] as well as on a single-molecule level.[40] The next complex electronic function of a two terminal single-molecule junction is switching, requiring a bistable molecular structure. Several triggers to alter between the molecules state were considered such as light, electrochemistry or the applied electrical field. Variation of the transport current due to single-molecule photoisomerization was observed for diarylethene[41] and azobenzene systems.[7] Transient electro-

[a] Department of Chemistry, University of Basel,
St. Johanns-Ring 19, 4056 Basel, Switzerland
Fax: +41-61-267-1016
E-mail: marcel.mayor@unibas.ch
[b] Department of Physics, University of Basel,
Klingelbergstrasse 82, 4056 Basel, Switzerland
E-mail: michel.calame@unibas.ch
[c] Karlsruhe Institute of Technology, Institute for Nanotechnology,
P. O. Box 3640, 76021 Karlsruhe, Germany
Supporting information for this article is available on the WWW under http://dx.doi.org/10.1002/ejoc.200901150.

chemically triggered single-molecule junctions were reported for immobilized redox active species like e.g. viologens[42–46] and ferrocenes.[47,48] Attempts to integrate electrochemically swithable supramolecular single-molecule systems were so far limited to a rotaxane in a platinum-based break junction.[49] Recently, even an example of a single-molecule switch based on the applied electric field was reported to display a weak hysteresis.[50] Unfortunately, the paper reports exclusively the phenomenon without a suggestion of the switching mechanism.

We have synthesized numerous model compounds to investigate hypothesized switching mechanisms in monomolecular films and on a single-molecule level ranging from optically addressed azobenzene systems[8,51,52] over electrochemically triggered viologens[44,46] and rigid rod cruciforms[53,54] to macrocyclic structures.[55,56] Recently we proposed to profit from the potential dependent coordination of pyridines to gold electrodes[17,57–59] as switching mechanism in an electrochemically controlled junction. A molecular cruciform consisting of two bars with different transport features and different terminal anchor groups was suggested.[53] As displayed in Figure 1, the lower conducting bar with sulfur anchor groups covalently immobilizes the molecule within the junction and the potential dependent coordination of the high conducting bar should provide a switching mechanism on a single-molecule level. While electrochemical control has already been achieved for transient single-molecule junctions,[17,44,46,60] the combination of stable single-molecule junctions at room temperature with electrochemical control allowing to switch an immobilized molecule remains challenging.

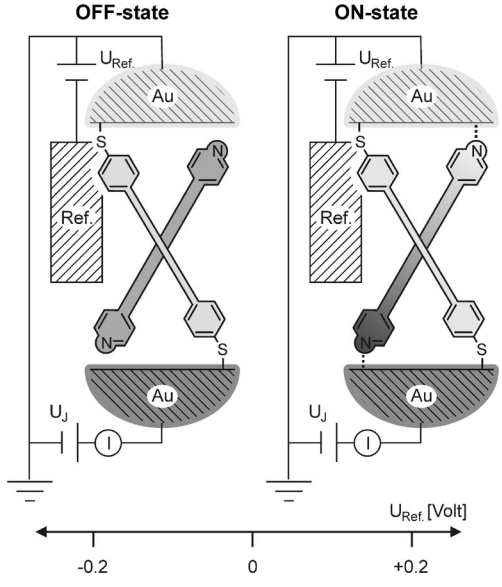

Figure 1. Coordination-induced switching principle: the coordination of the better conducting terminally pyridine-functionalized bar subunit to both electrodes is controlled by the electrochemical potential applied with respect to a reference electrode. Upon coordination (ON-state) the potential between both electrodes triggers electron transport through the bar subunit.

Cruciform molecules are not only interesting model compounds for molecular electronics.[54,61] Related structural motives were already investigated as electrooptically active chromophores in self-assembled thin films,[62,63] as chromophores with tuneable band gaps,[64] as metal ion[65–67] or pH[68]sensors,[69] and as building blocks of coordination polymers.[70]

The proposed switching mechanism relies on the different electronic transparencies of the bar subunits and the interplay of their anchor groups with the electrochemical potential. In our parent design (cruciform **1**) the sulfur anchor group was in *meta*-position to disfavour electronic communication through the sulfur immobilized bar.[71] However, the transport currents through this subunit were too little to enable its immobilization in a MCBJ in a liquid environment. Moving the sulfur anchor groups into *para*-positions (cruciform **2**) considerably increases the electronic transport through the immobilized molecule allowing to observe its presence within the junction. However, the increased transport through the sulfur-functionalized OPV bar considerably reduces the potential window to observe the coordination dependent switching of the pyridine-functionalized bar. We thus investigated systematically the single-molecule transport currents through the corresponding sulfur and pyridine-functionalized OPE and OPV rod subunits in the MCBJ setup in a liquid environment without electrochemical control.[33] The observed results are sketched in Figure 2.

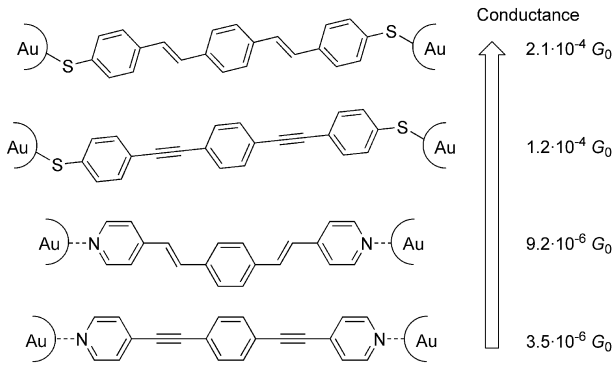

Figure 2. Measured trend in the conductivity of the OPV and OPE rods with terminal sulfur or pyridine anchor groups.

While the increased electron transport through the OPV structures with respect to the corresponding OPE structures was expected due to the superior overlap of the olefinic π-system with the phenyl π-system compared to the acetylene π-system, the improved conductivity of the sulfur immobilized rods compared to the pyridine-functionalized counterparts was surprising.[28,57] Consequently, the additional conductivity due to the coordination of the pyridine subunits of **2** can not be observed at a lower applied potential between the two electrodes than the transport current arising from the *para*-sulfur-functionalized OPV bar, making its detection very challenging.

To enable the suggested switching mechanism we currently follow two strategies. While from the side of the transport experiment we are working on increasing the sensitivity to enable the controlled immobilization of low conducting rods like the *meta*-sulfur-functionalized OPV subunit of the cruciform **1**, the chemical design and synthesis side works on favouring the expected transport features of the pyridine rod with respect to the sulfur-functionalized subunit. Along these lines we would like to report here the synthesis, the structural analysis and first transport investigations of the new cruciform structures **3** and **4** (Scheme 1) consisting of terminally pyridine-functionalized OPV rod subunits and perpendicular sulfur-functionalized oligophenylene (OP) type bar substructures.

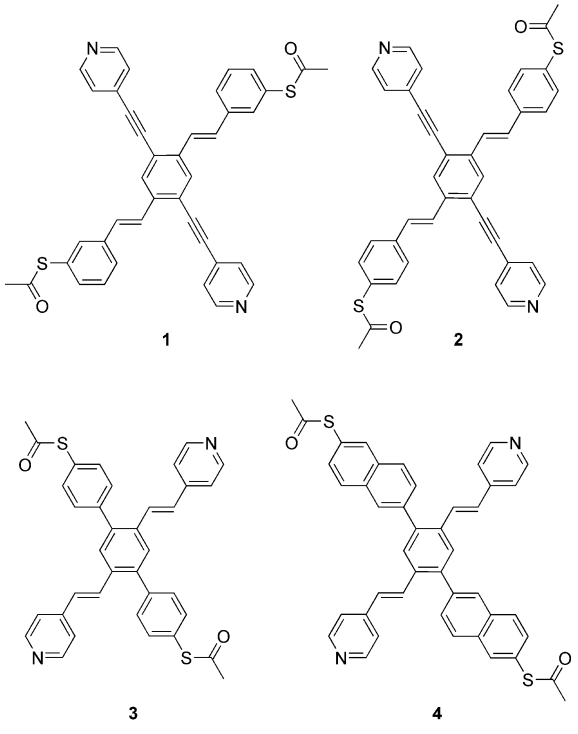

Scheme 1. First generation of OPV/OPE cruciforms **1** and **2** and the new OP/OPV cruciforms **3** and **4**.

Results and Discussion

Molecular Design

To favour the transport current through the pyridine-functionalized rod it consists of an OPV-type backbone in **3** and **4**. A considerable spatial mismatch was expected for a terminally sulfur-functionalized OPE rod. Furthermore, the sulfur anchor groups should again be in *meta*-position as the corresponding *para*-sulfur-functionalized OPE trimer displayed increased conductivity compared to the pyridine-functionalized OPV-type rod (see Figure 2). While we were able to measure electronic transport through individual molecules consisting of a comparable structural motive in ultra high vacuum (UHV),[71] the structure would again be clearly under our current detection limit in solution. Alternatively, a perpendicular oligophenylene (OP) type structure was considered. In particular OP structures comprising sterically repelling substituents *ortho* to the interring bridge position displayed rather limited transport features in a UHV MCBJ setup.[38] In the cruciform structures **3** and **4** the second OPV bar is placed in *ortho*-position with respect to the OP backbone and thus, a considerable increase in the interring torsion angle should result in a concomitant decrease in its transport properties. In the case of the cruciform **3**, the OP rod subunit is with about 1.5 nm between both terminal sulfur atoms slightly shorter than the pyridine-functionalized OPV bar, which has about 1.6 nm between both terminal pyridine nitrogen atoms. To enlarge the intramolecular sulfur–sulfur distance of the OP-type bar both terminal phenyl units of **3** have been replaced by naphthyl units in **4**, expanding the length of the OP backbone to about 1.9 nm.

Synthetic Strategy

The synthetic strategy is to build up first the OPV system by a Horner–Wadsworth–Emmons (HWE) reaction. The perpendicular OP system will be assembled by a Suzuki reaction with the corresponding boronic acid derivatives. As the terminal sulfur anchor groups are already present during the aryl coupling reaction, ethyl-TMS-protected sulfur precursors are considered. The ethyl-TMS protection group was already reported to maintain the basic conditions of a Sonogashira reaction[72] and can be transprotected to the desired acetyl protection group under rather mild reaction conditions. Thus, an ethyl-TMS-protected thiophenol seemed ideally suited to survive Suzuki cross coupling reaction conditions as well.

Synthesis

The functional OPV building block **5** was synthesized following a reported procedure.[73] With its two iodine atoms as excellent leaving groups in palladium catalyzed coupling reactions, compound **5** is an ideal candidate for a Suzuki reaction to assemble the OP system. Thus, the corresponding sulfur bearing boronic acid is required. The corresponding boronic acid **8** was synthesized starting from 4-bromothiophenol (**6**) (Scheme 2). The thiol **6** reacts in a radical addition reaction with vinyltrimethylsilane, using *tert*-butyl peroxide as radical initiator, to the ethyl-TMS-protected thiol **12** in 67% yield.[72] Subsequently, the boronic acid was introduced by treating compound **7** with a 1.6 M solution of *n*-butyllithium (*n*BuLi) in hexane to perform a bromine–lithium exchange.[72] The lithiated intermediate is quenched by triisopropyl borate to provide boronic acid **8** as a colourless solid after aqueous work up in 59% yield.

Having all building blocks for the assembly of the framework for the new cruciform structure in hand, its synthesis was investigated. Diiodo derivative **5** and boronic acid **8** were dissolved in a toluene/ethanol mixture to which cata-

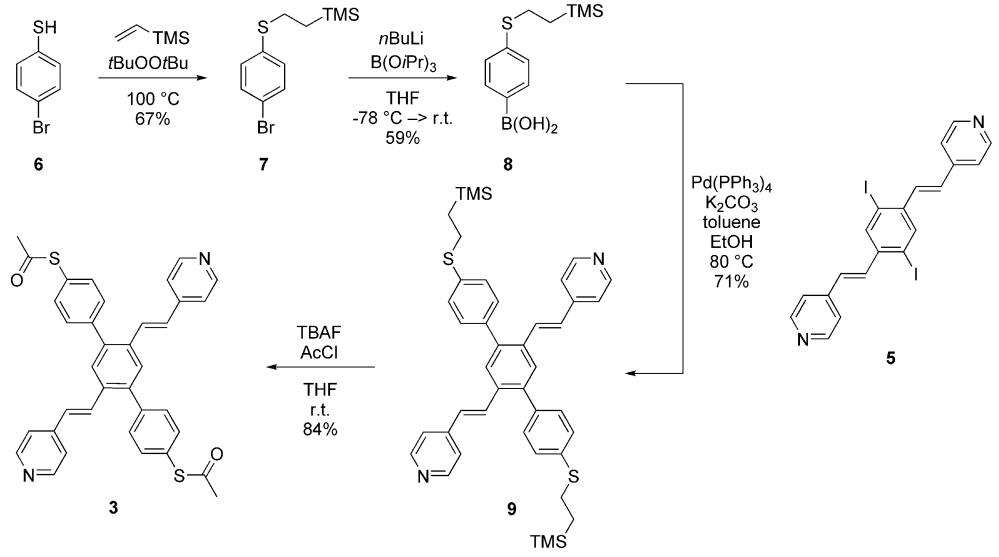

Scheme 2. Synthesis of target structure **3**.

lytic amounts of tetrakis(triphenylphosphane)palladium and an excess (3.6 equiv.) of potassium carbonate (K_2CO_3) as base was added. After stirring for 7.5 h at 80 °C followed by aqueous work up the crude was purified by column chromatography (CC) to provide the cruciform structure **9** as a yellow solid in 71% yield. The final step is the transprotection from the ethyl-TMS masked to acetyl-protected sulfur anchor groups. While the ethyl-TMS group was easily cleaved by tetrabutylammonium fluoride (TBAF) the subsequent treatment with acetyl chloride (AcCl) resulted in the acetylation of both, the sulfur groups and the pyridine nitrogen atoms. Fortunately, the intense study of Karl Freudenberg and Daniel Peters[74] revealed that acetylated pyridine units are fast and efficiently cleaved by their treatment in chloroform ($CHCl_3$) with ethanol (EtOH).[74] Thus, the ethyl-TMS-protected compound **9** was dissolved in tetrahydrofuran (THF) to which a TBAF solution was added. After stirring for 1 h at room temperature (room temp.), an excess of AcCl was added at 0 °C. The reaction mixture was stirred for 30 min while warming to room temp. Subsequently, $CHCl_3$ and EtOH were added. After aqueous work up and CC the cruciform **3** was isolated in 84% yield as a yellow solid.

For the assembly of target structure **4** boronic acid **16** was required (Scheme 3). Our strategy was to introduce the sulfur via a Newman–Kwart rearrangement (NKR) as ef-

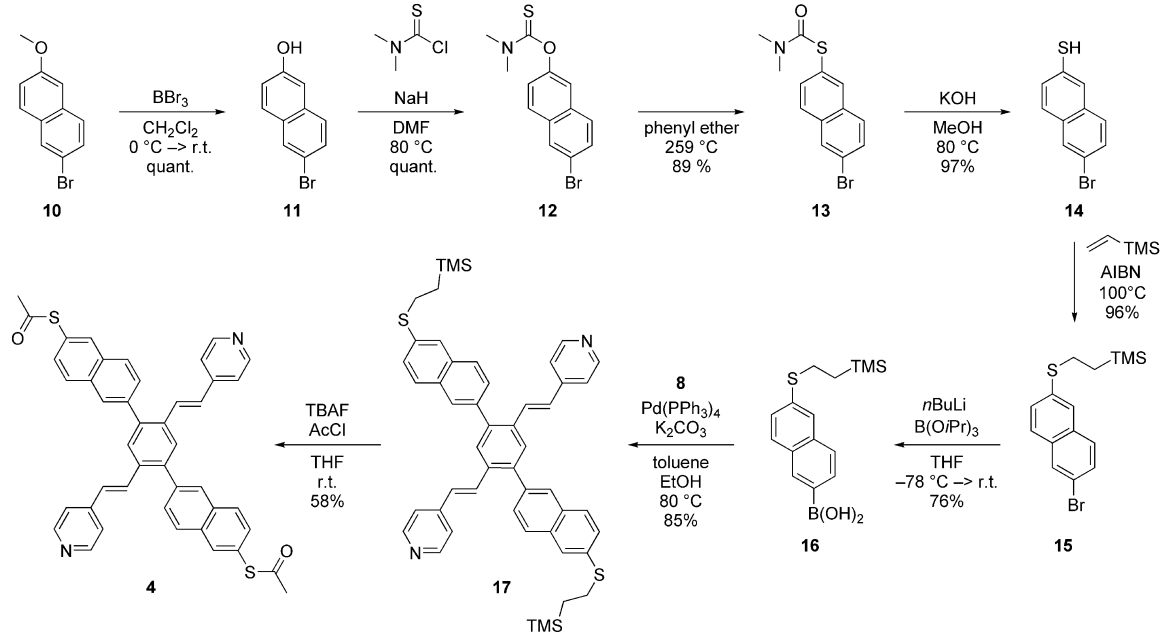

Scheme 3. Synthesis of target structure **4**. After deprotecting 2-bromo-6-methoxynaphthalene the phenol is converted to a thiophenol via a Newman–Kwart rearrangement. Protection of the thiol and formation of the boronic acid leads to the building block **16** needed for the Suzuki reaction to assemble the cruciform structure.

ficient method to convert phenols to thiophenols by the thermally activated rearrangement of an *O*-thiocarbamate to the corresponding *S*-thiocarbamate.[75–77] The *O*-thiocarbamate **12** was synthesized by treating 6-bromonaphthalen-2-ol (**11**), available after deprotection of 2-bromo-6-methoxynaphthalene (**10**) with BBr_3, with dimethylcarbamoyl chloride using sodium hydride (NaH) as base.[78] The *O*-thiocarbamate **12** was dissolved in diphenyl ether and heated to 259 °C. The extent of the rearrangement of **12** to the *S*-thiocarbamate **13** was monitored by thin-layer chromatography (TLC). After 1.5 h the reaction mixture was cooled to room temp. and directly exposed to CC to provide the *S*-thiocarbamate **13** as a beige solid in 89% yield. After hydrolysis with KOH in methanol, 6-bromonaphthalene-2-thiol (**14**) was obtained as a beige solid in 97% yield. The thiol **14** was ethyl-TMS-protected by heating it to 100 °C in vinyltrimethylsilane and traces of 2,2′-azobis(2-methylpropionitrile) (AIBN) as radical starter in a pressure tube. Upon cooling down, the ethyl-TMS-protected thionaphthalene derivative **15** was obtained as a beige precipitate in 96% yield. Treating **15** with *n*BuLi in dry THF at –78 °C and quenching with triisopropyl borate followed by an aqueous work up and recrystallization from hexane provided boronic acid **16** as a beige solid in 76% yield. For the Suzuki coupling of the new boronic acid **16** with diiodo derivative **5**, similar reaction conditions were applied as described above for boronic acid **8**. The new cruciform **17** comprising ethyl-TMS protection groups was isolated in 85% yield as a yellow solid after CC. For the transprotection of the sulfur, similar reaction conditions as described above for the cruciform **9** were applied to **17**. Thus, after deprotection with TBAF and treating with

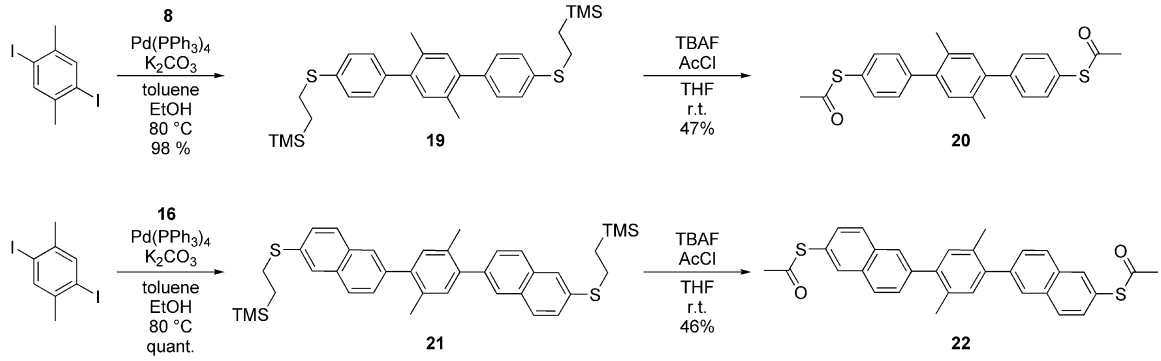

Scheme 4. Synthesis of control molecules **20** and **22**.

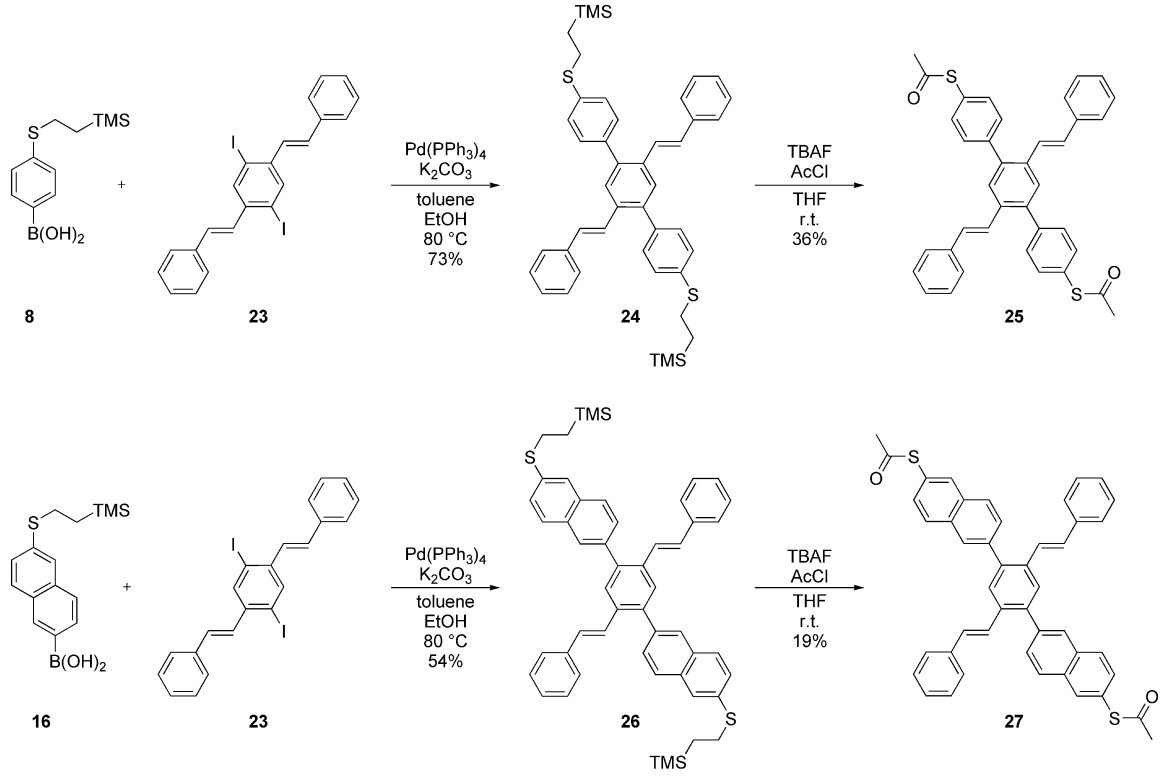

Scheme 5. Synthesis of control molecules **25** and **27**.

AcCl, followed by hydrolysis in the $CHCl_3$/EtOH, purification by CC provided the acetyl-protected cruciform **4** as a yellowish solid in 58% yield (Scheme 3).

Both target cruciforms **3** and **4** were successfully synthesized. To be able to relate particular transport characteristics to the rod-like subunits of the cruciforms, several control compounds either consisting of a single bar of the cruciform structure or lacking the coordinating pyridine nitrogen atom have been synthesized in addition. Thus, the OPV with two pyridine anchor groups **18** was synthesized following a reported procedure.[79] Furthermore, the corresponding oligoaryl rods **20** and **22** were assembled to mimic the terminal sulfur-functionalized bar substructure.

Therefore **20** and **22** were assembled via a Suzuki reaction. The corresponding boronic acid was treated with 2,6-diiodo-*p*-xylene to give the rods **19** and **21**, respectively. Transprotection of the sulfur using the same conditions as described above yielded the acetylated control molecules **20** and **22**, respectively (Scheme 4).

Further the two cruciform structures without pyridine anchor groups but terminal benzene units at the transversal bar substructure **25** and **27** were synthesized. Therefore the iodinated OPV bar **23** was synthesized by a reported procedure.[64] Having both building blocks, diiodide **23** and boronic acids **8** and **16**, respectively, in hand, the assembly of the control cruciforms was achieved by using similar protocols as already described. Again, a Suzuki coupling reaction followed by a transprotection of the sulfur unit yielded the desired control molecules **25** and **27** (Scheme 5).

All new compounds were analyzed by determination of the melting point (if solids), determination of the R_f value, ^1H NMR and ^{13}C NMR spectroscopy, mass spectrometry and elemental analysis (EA). Further UV/Vis spectra of all cruciform structures **3**, **4**, **9**, **17**, **25** and **27** such as of the corresponding rods **20** and **22** were recorded. Interestingly, in spite of numerous different purification attempts, we were not able to record correct EA data of all target cruciform structures. Gel permeation chromatography (GPC) in a HPLC setup was performed and the GPC chromatograms of compound **3**, **4**, **20**, **22**, **25** and **27** are provided in the SI.

Single-Molecule Transport Investigations

The above described target structures were investigated in a mechanically controllable break junction (MCBJ) setup described previously.[19,32,33,53] The principle of a MCBJ is depicted in Figure 3. A gold lead with a free-standing constriction in its middle (80–150 nm wide) is fabricated on an electrically isolated, flexible spring-steel substrate. By mounting the substrate in a three point bending mechanism, the constriction can be stretched and eventually broken. This results in two atomic gold tips, which can be brought back into contact by relaxing the bending tension of the substrate. When broken in the presence of molecules with anchoring groups, the two tips form ideal electrodes to contact single molecules. The gap distance *d* between the electrodes can be adjusted by controlling the pushrod position. During a typical experiment, the pushrod is moved at a velocity of ca. 30 μm/s, so that the two gold leads separate at ca. 1 nm/s.

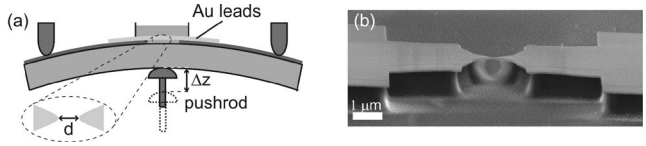

Figure 3. (a) Schematics of the MCBJ principle with a liquid cell. (b) SEM image of the central part of a microfabricated Au junction on top of a polyimide-coated stainless-steel substrate.

In order to measure in a liquid environment, a liquid cell (cell volume: 3 mL) is integrated into the setup. The cell consists of a Viton tube placed on top of the break junction sample and a larger glass reservoir, which allows an efficient delivery of the molecules to the Au electrodes. Transient molecular junctions are formed by periodically opening and closing the Au junction in the presence of molecules in solution. Typically, target molecules are dissolved in a mixture of THF and mesitylene (1:4 v/v, henceforth referred to as the solvent) to a final concentration of 0.25 mM. In order to remove the acetyl protection groups, a 50 mM tetrabutylammonium hydroxide (TBAH) deprotecting agent was added to the solution. During the measurements the solution was kept under an argon protection gas atmosphere to exclude oxygen, as molecular rods comprising two terminal thiophenols are prone to polymerization by disulfide formation in the presence of oxygen. To determine the electrical conductance *G* of the molecular junctions, a voltage bias of 0.2 V is applied between the left and right contacts, and the resulting current is measured with a custom made autoranging IV converter. By recording hundreds of conductance traces, a statistical analysis can be done and an average conductance of the junction deduced.[32] The measured conductance traces are converted to a logarithmic scale and the $\log(G)$ histogram is calculated using a constant bin size. This representation gives a better overview (over six orders of magnitude) of the molecular junction conductance. Typically, a set of 100 single conductance curves was used to calculate one histogram. The peak position and shape of the conductance histogram are interpreted as the typical signature of a particular molecule.

First, cruciform **3** was exposed to the break junction without adding any deprotection agent (Figure 4, a). Quite remarkably, the signature of compound **3** shows two distinct peaks.[80] In contrast, when compound **3** is deprotected in the liquid cell, then only the peak with higher conductivity is observed (Figure 4, b). As the spontaneous deprotection of the sulfur anchor group in the presence of Au electrodes is expected, the observation of two peaks points towards the formation of junctions bridged by the sulfur-functionalized OP bar and by the pyridine-functionalized OPV bar with comparable probabilities. Upon chemical deprotection of the sulfur anchor group in solution, the molecular junction bridged by the immobilization of the OP rod with terminal sulfur groups seemed to be favoured. To clarify this point, we further investigated the rod-like sub-

units of compound **3**, namely the sulfur-functionalized OP rod **20** and the pyridine OPV bar **18** *separately* (Figure 4, c and d, respectively). These experiments support the view that the two peaks observed in part a of Figure 4 for the still protected compound **3** stem from the two rods forming the cruciform structure. We expect that the pyridine OPV rod of compound **3** can be immobilized between the two electrodes, giving rise to the peak at lower conductance. However, in this situation, the protected sulfur end comes close to the Au electrodes as well. Because the OP rod cannot diffuse freely in solution, the probability to have a spontaneous deprotection of the sulfur groups increases: we will sometimes form a sulfur–gold covalent bond at both ends of the OP rod. If this spontaneous deprotection happens frequently enough, we expect the system to present two possible stable local conformations for the molecular junction: one where the pyridine OPV rod dominates transport and one where the thiolated OP rod dominates. By deprotecting the sulfur end groups, we simply shift the equilibrium of the system towards the situation dominated by the OP rod. This interpretation is qualitatively supported by the control measurements performed for the rods taken separately. Indeed, the peak for the pyridine OPV **18** appears clearly at a substantially lower conductance than that for the deprotected OP rod **20**, the latter being close to the peak exhibited by the deprotected compound **3**. Note also that measurements of the OP rod **20** when still protected do not exhibit a molecular signature: the probability for spontaneous deprotection is here too low to result in a clear signal. The conductance histogram in this case is similar to that for the pure solvent (Figure 4, h). An overview of the peak conductance values in the log(*G*) histograms is provided in Table 1. $G_{\text{log-low}}$ and $G_{\text{log-high}}$ are obtained by a Gaussian fit of the molecular peak in the log(*G*)–conductance histograms. $G_{\text{lin-low}}$ and $G_{\text{lin-high}}$ are the same conductance values transformed to a linear scale. Due to the width of the peaks and the log scale, the G_{lin} values are slightly shifted to lower conductances.[33]

Table 1. Conductance values of the measured compounds. G_{log} denote the values derived from a Gaussian fit of the molecular signature in the log(*G*) histogram. G_{lin} denotes the corresponding maximum in a linear representation, which results slightly shifted to lower values, depending on the width of the peak in log scale.[33]

Molecule	$G_{\text{log-low}}$ [G_0]	$G_{\text{log-high}}$ [G_0]	$G_{\text{lin-low}}$ [G_0]	$G_{\text{lin-high}}$ [G_0]
3 – protected	–5.1	–3.8	3.3×10^{-6}	9.8×10^{-5}
3 – deprotected		–3.6		1.5×10^{-4}
4 – protected	–4.8	–4.3	9.9×10^{-6}	2.6×10^{-5}
4 – deprotected		–4.5		1.9×10^{-5}
18	–4.7		9.2×10^{-6}	
20 – deprotected		–3.8		6.2×10^{-5}
22 – deprotected		–4.4		1.6×10^{-5}

Cruciform **4** was also investigated in the MCBJ and a similar pattern in the histogram is observed. When no deprotection agent is added (Figure 4, e), two peaks appear, while when the cruciform is first deprotected, only one distinct peak is observed (Figure 4, f). Again, comparison with the parent rod subunits **22** and **18** displayed that the lower peak corresponds well to that of the pyridine OPV **18** (Figure 4, d) and the higher peak to that of the single rod **22** (Figure 4, g). However, the two peaks of **4** in Figure 4, e, are less clearly separated than what was observed for compound **3**, pointing at the lower conductance of the sulfur terminated rod subunit of the cruciform **4** compared to **3** (see Table 1). It is therefore not surprising that cruciform **4** shows a slightly lower conductance than the previously investigated cruciforms **2** and **3**.

For both cruciform structures **3** and **4** the sulfur terminated OP-type rod is better conducting than the pyridine-functionalized OPV rod, making the observation of the co-

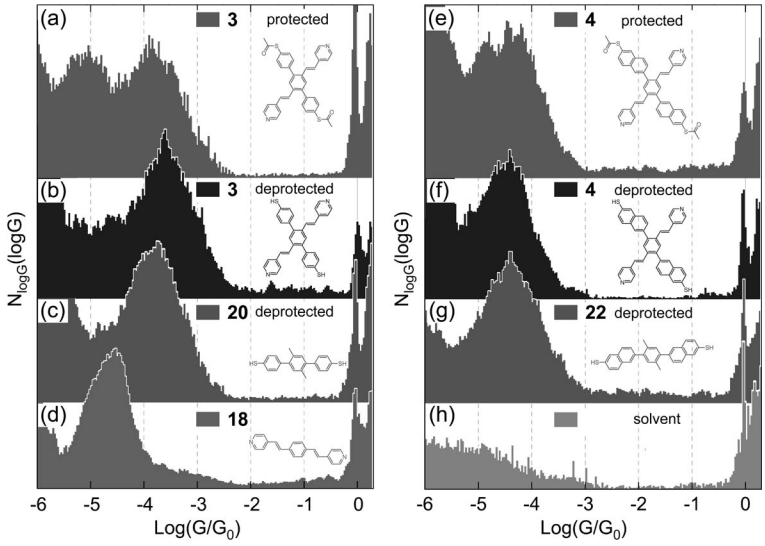

Figure 4. Measured conductance histograms for compounds **3** and **4** without and with deprotection agent (a), (b) and (e), (f). The measured reference conductance histograms for compounds **20**, **18**, **22**, as well as for the solvent alone are shown in (c), (d), (g) and (h), respectively.

ordination-induced switching challenging. In particular for the cruciform **4**, the proximity of the signature of both rods will make the detection of the coordination-induced switching of its OPV subunit very demanding. We expect that applying a potential to the liquid cell in the appropriate conditions shall enable us to modulate the conductance of the pyridine-functionalized OPV (**18**) by adjusting the pyridine–gold coordination.[17,57–59] Ultimately a binding-unbinding control of the pyridine rod shall be possible. By doing this, the signature of the molecular junction shall alternate between a single and a double peak, thereby revealing a switching mechanism between a state where both rods can bind (as shown in Figure 4, a and e) or where exclusively the sulfur-terminated rod binds (see Figure 4, b and f).

Further experiments are now underway where the possible switching effects of the cruciform molecules are being investigated. For this purpose, a modified MCBJ setup including a potentiostat for proper electrochemical control has been developed. Detailed results of these experiments will be published elsewhere.

Conclusions

Two new families of cruciforms, **3** and **4**, based on a pyridine-functionalized OPV rod and transversal sulfur-functionalized OP-type rod were designed and synthesized as potential coordination-induced single-molecule switches. Their assembly was based on Horner–Wadsworth–Emmons reactions and Suzuki cross-coupling chemistry. For the OP-type substructure, the required boronic acid derivatives comprising ethyl-TMS-protected sulfur groups were synthesized. Interestingly, the ethyl-TMS-protected thiophenols were stable under the basic reaction conditions of the Suzuki reaction even at elevated temperature and were efficiently transprotected to the acetyl-protected thiophenols required for the immobilization strategy. In addition, several control molecules like the pyridine-functionalized OPV bar **18**, both acetylsulfanyl-functionalized OP-type rods **20** and **22**, together with cruciform structures **25** and **27** lacking the coordinating pyridine nitrogen atoms, were synthesized.

Transport investigations through these new cruciforms and the corresponding control molecules were performed in a MCBJ setup in a liquid environment. All cruciforms and control structures were immobilized at a single-molecule level, and their transport signature was recorded. We could demonstrate that both rods of the cruciform structures are functional and can be used for immobilization. Control experiments of the separate building blocks of the cruciform were also performed to carefully characterize the functional compound and confirm the immobilization of the cruciform. In spite of the new design, the *para*-sulfur-functionalized OP-type rod remained the transport-dominating substructure. However, when the coordination of the sulfur to the gold electrode is handicapped by acetyl protection groups, the signature of both bar substructures (the OP-type rod and the pyridine-functionalized OPV rod) were recorded. Detailed investigations of the behaviour of the cruciform in the presence of a control potential within an electrochemical break junction setup are currently underway.

The switching concept originally developed aimed at an increase in conductance upon coordination of the pyridine bar. We now observed experimentally that the pyridine rod exhibits a lower conductance than the sulfur bar. The molecular system will therefore not result in an overall increase in conductance of the molecular junction upon coordination. This, however, does not prevent the switching of the cross to be detected. As indeed demonstrated above, the signature of the cross can be tuned to present a stark contrast between its two possible conformational states between the electrodes. By choosing rods with sufficiently separated conductances, as is the case for compound **3**, we expect to be able to unambiguously determine the binding status of the cross within the junction. Current efforts aim at synthesizing alternative cruciform structures as well as improving the detection electronics to improve the signal-to-noise ratio between the conductances of the different binding states of the cross compound.

Experimental Section

Reagents and Solvents: All chemicals were used for the synthesis without further purification unless otherwise noted. The solvents for chromatography and crystallization were distilled once before use, the solvents for extraction were used in technical grade. Dry tetrahydrofuran (THF) and dry dichloromethane (DCM) were dispensed from a Pure Solv MD Solvent Purification System. Dry toluene was distilled from Na/benzophenone. Dry DMF was purchased over molecular sieves from Fluka.

Synthesis: All reactions with reagents, which are easily oxidized or hydrolyzed, were performed under argon using Schlenk technique, only dry solvents were used and the glassware was heated out.

Analytics and Instruments: Bruker DPX NMR (400 MHz) and Bruker BZH NMR (250 MHz) instruments were used to record the ^{1}H NMR spectra. Chemical shifts (δ) are reported in parts per million (ppm) relative to residual solvent peaks or trimethylsilane (TMS), and coupling constants [J] are reported in Hertz [Hz]. NMR solvents were obtained from Cambridge Isotope Laboratories, Inc. (Andover, MA, USA). The measurements were done at room temperature. Bruker DPX NMR (101 MHz) instruments were used to record the ^{13}C NMR spectra. Chemical shifts (δ) are reported in parts per million (ppm) relative to residual solvent peaks. The measurements were done at room temperature. Mass spectra were recorded with a Bruker esquire 3000 plus (for ESI), a Finnigan MAT 95Q (for EI), a Finnigan MAT 8400 (for FAB), or a Voyger-De™ Pro (for MALDI-TOF) instrument. Elementary analyses were performed with a Perkin–Elmer Analysator 240. UV/Vis spectroscopy was measured in DCM with an Agilent 8453 instrument. Gel permeation chromatograms were recorded with a Shimadzu LC-8A chromatograph. The measurements were done at room temperature with an OligoPore 300 × 7.5 mm column (particle size 6 μm) from Polymer Laboratories, by eluting with toluene with a flow rate of 0.5 mL/min at λ = 220 nm. For column chromatography, silica gel 60 (40–63 μm) from Merck or silica gel 60 (40–63 μm) from Fluka was used. For TLC silica gel 60 F_{254} glass plates with a thickness of 0.25 mm from Merck were used. UV light (254 or 366 nm) was used for detection.

4-[2-(Trimethylsilyl)ethylthio]phenylboronic Acid (8):[81] Bromide **7** (10.0 g, 34.6 mmol) was dissolved in dry THF (40 mL) in a 100 mL Schlenk flask and treated with *n*BuLi (1.6 M in hexane, 34.6 mL, 55.4 mmol) at –78 °C. It was stirred for 30 min before triisopropyl borate (41.4 mL, 180 mmol) was added. The reaction mixture was then stirred for 2 h at –78 °C, 2 h at –20 °C and 17 h at room temp. and then extracted with TBME (200 mL) and water (200 mL). The aqueous phase was washed with TBME (100 mL), the combined organic phases were washed with brine (2 × 100 mL), dried with $MgSO_4$, filtered and the solvents evaporated. The crude was recrystallized from hexane to give a colourless solid (5.20 g, 20.5 mmol, 59%); m.p. 144.3–145.5 °C. ^{1}H NMR (400 MHz, $CDCl_3$, 25 °C): δ = 8.10 [d, ^3J(H,H) = 8.2 Hz, 2 H, CH], 7.36 (d, $^3J_{H,H}$ = 8.2 Hz, 2 H, CH), 3.05 (m, 2 H, CH_2), 1.00 (m, 2 H, CH_2), 0.09 (s, 9 H, $SiMe_3$) ppm. ^{13}C NMR (101 MHz, $CDCl_3$, 25 °C): δ = 143.7, 135.9, 126.4, 28.1, 16.6, –1.8 ppm. MS (MALDI-TOF): found *m*/*z* = 254.94, 254.10 calculated for $C_{11}H_{19}BO_2SSi$.

1,4-Bis{4-[2-(trimethylsilyl)ethylthio]phenyl}-2,5-bis[(*E*)-pyridin-4-ylvinyl]benzene (9): Iodide **5** (99.0 mg, 0.185 mmol) and boronic acid **8** (103 mg, 0.406 mmol) were dissolved in toluene (7 mL) and ethanol (2 mL). The mixture was degassed for 10 min, before K_2CO_3 (205 mg, 1.48 mmol) and $Pd(PPh_3)_4$ (20.0 mg, 0.0173 mmol) was added. It was then stirred for 7.5 h at 80 °C. The hot reaction mixture was filtered, washed with toluene, evaporated and purified by column chromatography (silica gel, 2 × 12 cm, CH_2Cl_2, 1% MeOH) to give compound **9** as a colourless solid (92.0 mg, 0.131 mmol, 71%); m.p. 158.5 –160.0 °C. TLC R_f = 0.34 (CH_2Cl_2, 5% MeOH). ^{1}H NMR (400 MHz, $CDCl_3$, 25 °C): δ = 12.80 (m, 4 H), 7.74 (s, 2 H), 7.43–7.33 (m, 10 H), 7.22 (m, 4 H), 7.02 (d, $^3J_{H,H}$ = 16.2 Hz, 2 H), 3.06 (m, 4 H, CH_2), 1.02 (m, 4 H, CH_2), 0.09 (s, 18 H, $SiMe_3$) ppm. ^{13}C NMR (101 MHz, $CDCl_3$, 25 °C): δ = 150.2, 144.5, 140.5, 137.5, 136.9, 134.4, 131.3, 130.2, 128.1, 128.0, 127.4, 120.9, 29.1, 16.8, –1.7 ppm. MS (EI): *m*/*z* (%) = 700.3 (24) [M$^+$], 672.3 (17), 644.3 (6), 73.0 (100). GPC (oligopore 6 µm, toluene, UV/Vis photodiode array detector) area 100%. UV/Vis: λ_{max} 280, 310, 342 nm.

1,4-Bis(4-thioacetylphenyl)-2,5-bis[(*E*)-pyridin-4-ylvinyl]benzene (3): The starting material **9** (122 mg, 0.174 mmol) was dissolved in dry THF (20 mL) in a 100 mL flask and the solution was saturated with argon. Then TBAF (1 M in THF, 3 mL, 3 mmol) was added and it was stirred for 1 h at room temperature. To the pinkish solution was then added acetyl chloride (0.4 mL, 4.6 mmol) at 0 °C. The reaction mixture turned yellow and was stirred for 30 min at room temperature. Then chloroform (15 mL) and ethanol (15 mL) were added. The reaction mixture was extracted with dichloromethane and water, the aqueous phase was washed three times with dichloromethane, the combined organic phases were washed with brine, dried with $MgSO_4$ and the solvents evaporated. The crude was purified by column chromatography (silica gel, 1 × 12 cm, CH_2Cl_2, 1% MeOH) to give the product **3** as a yellow solid (85 mg, 0.145 mmol, 84%); m.p. 208.4–210.9 °C. TLC R_f = 0.18 (CH_2Cl_2, 5% MeOH). ^{1}H NMR (400 MHz, $CDCl_3$, 25 °C): δ = 8.54 (m, 4 H), 7.78 (s, 2 H), 7.56 (d, $^3J_{H,H}$ = 8.2 Hz, 4 H), 7.51 (d, $^3J_{H,H}$ = 8.2 Hz, 4 H), 7.32 (d, $^3J_{H,H}$ = 16.3 Hz, 2 H), 7.23 (m, 4 H), 7.03 (d, $^3J_{H,H}$ = 16.2 Hz, 2 H), 2.50 (s, 6 H, CH_3) ppm. ^{13}C NMR (101 MHz, $CDCl_3$, 25 °C): δ = 193.8, 150.3, 144.3, 140.9, 140.4, 134.5, 134.4, 130.7, 130.5, 128.2, 128.1, 127.6, 120.9, 30.4 ppm. MS (MALDI-TOF): found *m*/*z* = 584.91, 584.16 calculated for $C_{36}H_{28}N_2O_2S_2$. GPC (oligopore 6 µm, toluene, UV/Vis photodiode array detector) area 99.9%. UV/Vis: λ_{max} = 291, 342 nm.

2,5-Bis{4-[2-(trimethylsilyl)ethylthio]phenyl}-*p*-xylene (19): Boronic acid **8** (389 mg, 1.53 mmol) was dissolved in toluene (20 mL) and ethanol (5 mL). The mixture was degassed for 10 min before 2,5-diiodo-*p*-xylene (232 mg, 0.648 mmol), $Pd(PPh_3)_4$ (160 mg, 0.139 mmol) and K_2CO_3 (850 mg, 6.15 mmol) were added. The reaction mixture was then stirred for 14 h at 80 °C, cooled to room temp. and extracted with TBME and water. The aqueous phase was washed with TBME. The combined organic phases were washed with water and brine, dried with $MgSO_4$, evaporated and purified by CC (silica gel, 3 × 12 cm, hexane/EtOAc = 20:1) to give **19** as a colourless solid (331 mg, 0.633 mmol, 98%); m.p. 116.6–117.4 °C. TLC R_f = 0.40 (hexane/EtOAc = 20:1). ^{1}H NMR (400 MHz, $CDCl_3$, 25 °C): δ = 7.36 (d, $^3J_{H,H}$ = 8.5 Hz, 4 H), 7.30 (d, $^3J_{H,H}$ = 8.5 Hz, 4 H), 7.15 (s, 2 H), 3.03 (m, 4 H, CH_2), 2.29 (s, 6 H, Me), 0.99 (m, 4 H, CH_2), 0.07 (s, 18 H, $SiMe_3$) ppm. ^{13}C NMR (101 MHz, $CDCl_3$, 25 °C): δ = 140.2, 139.0, 135.8, 132.6, 131.8, 129.6, 128.3, 29.5, 19.9, 16.9, –1.7 ppm. MS (EI): *m*/*z* (%) = 522.3 (33) [M$^+$], 73.0 (100).

2,5-Bis(4-thioacetylphenyl)-*p*-xylene (20): The starting material **19** (41 mg, 0.0784 mmol) was dissolved in 5 mL of THF. The mixture was degassed for 15 min before TBAF (1 M in THF, 3.00 mL, 3.00 mmol) was added at room temp. The reaction mixture was stirred for 45 min, then acetyl chloride (1.50 mL, 21.0 mmol) was added at 0 °C. After stirring for 15 min at 0 °C, the reaction mixture was quenched with ice and extracted with DCM/water. The aqueous phase was washed twice with DCM. The combined organic phases were washed twice with water, dried with $MgSO_4$ and the solvents evaporated. The crude was purified by column chromatography (silica gel, 1 × 12 cm, hexane/EtOAc = 20:1) to give **20** as a colourless solid (15 mg, 0.0369 mmol, 47%); m.p. 190.5–195.8 °C. TLC R_f = 0.10 (hexane/EtOAc = 20:1). ^{1}H NMR (400 MHz, $CDCl_3$, 25 °C): δ = 7.48 (d, $^3J_{H,H}$ = 8.4 Hz, 4 H), 7.42 (d, $^3J_{H,H}$ = 8.4 Hz, 4 H), 7.17 (s, 2 H), 2.47 (s, 6 H, CH_3), 2.29 (s, 6 H, Me) ppm. ^{13}C NMR (101 MHz, $CDCl_3$, 25 °C): δ = 194.1, 142.7, 140.1, 134.1, 132.7, 131.9, 130.0, 126.3, 30.2, 19.9 ppm. MS (EI): *m*/*z* (%) = 406.1 (39) [M$^+$], 364.1 (26), 322.1 (100), 43 (14). GPC (oligopore 6 µm, toluene, UV/Vis photodiode array detector) area 99.8%. UV/Vis: λ_{max} = 273 nm.

***O*-(6-Bromonaphthalene-2-yl) Dimethylcarbamothioate (12):** 6-Bromonaphthalen-2-ol (500 mg, 2.24 mmol) was dissolved in DMF (10 mL) and added to a solution of sodium hydride (55% moistened with oil, 193 mg, 6.72 mmol) in DMF (8 mL) at 0 °C. The ice bath was taken away and the mixture stirred for 30 min. Then dimethyl carbamoyl chloride (830 mg, 6.72 mmol) was added and it was stirred for 2 h at 80 °C and 15 h at room temperature. The reaction mixture was then extracted with 1% aqueous NaOH (100 mL) and TBME (100 mL). The aqueous phase was washed with TBME (2 × 50 mL). The combined organic phases were washed with brine and 5% aqueous HCl (100 mL), dried with $MgSO_4$ and the solvents evaporated. The crude was purified by column chromatography (silica gel, 3 × 12 cm, CH_2Cl_2/hexane = 5:1) to give the thiocarbamate **12** as a colourless solid (695 mg, 2.24 mmol, 100%); m.p. 126.9–131.9 °C. TLC R_f = 0.43 (CH_2Cl_2/hexane = 5:1). ^{1}H NMR (400 MHz, $CDCl_3$, 25 °C): δ = 8.00 (s, 1 H), 7.75 (d, $^3J_{H,H}$ = 8.9 Hz, 1 H), 7.67 (d, $^3J_{H,H}$ = 8.7 Hz, 1 H), 7.54 (d, $^3J_{H,H}$ = 8.8 Hz, 1 H), 7.46 (s, 1 H), 7.27 (m, 1 H), 3.48 (s, 3 H, CH_3), 3.39 (s, 3 H, CH_3) ppm. ^{13}C NMR (101 MHz, $CDCl_3$, 25 °C): δ = 188.0, 152.3, 133.0, 132.5, 130.3, 129.8, 128.5, 124.1, 120.0, 43.8, 39.2 ppm. MS (EI): *m*/*z* (%) = 310.9 (17) 309.0 (16) [M$^+$], 88.0 (100). $C_{13}H_{12}BrNOS$ (310.21): calcd. C 50.33, H 3.90, N 4.52; found C 50.10, H 3.80, N 4.30.

***S*-(6-Bromonaphthalene-2-yl) Dimethylcarbamothioate (13):** Compound **12** (4.70 g, 15.2 mmol) and phenyl ether (20.0 g) were placed in a 100 mL two-necked flask with condenser (dry, Ar) and it was heated to reflux (259 °C) for 1.5 h. The reaction mixture was then

cooled to room temperature and directly chromatographed (silica gel, 4 × 12 cm, hexane/EtOAc = 5:1 to 3:1) to give **13** as a beige solid (4.20 g, 13.5 mmol, 89%); m.p. 106.5–108.2 °C. TLC R_f = 0.20 (hexane/EtOAc = 5:1). ^{1}H NMR (400 MHz, $CDCl_3$, 25 °C): δ = 8.00 (d, $^2J_{H,H}$ = 1.7 Hz, 1 H), 7.98 (s, 1 H), 7.75 (d, $^3J_{H,H}$ = 8.6 Hz, 1 H), 7.68 (d, $^3J_{H,H}$ = 8.8 Hz, 1 H), 7.57 (dd, $^2J_{H,H}$ = 1.8, $^3J_{H,H}$ = 8.6 Hz, 1 H), 7.56 (dd, $^2J_{H,H}$ = 2.0, $^3J_{H,H}$ = 8.7 Hz, 1 H), 3.13 (s, 3 H, CH_3), 3.04 (s, 3 H, CH_3) ppm. ^{13}C NMR (101 MHz, $CDCl_3$, 25 °C): δ = 166.6, 135.1, 134.2, 133.3, 131.8, 129.8, 129.7, 129.5, 127.4, 126.8, 121.0, 36.9 ppm. MS (EI): *m*/*z* (%) = 311.0 (8) 309.0 (8) [M$^+$], 158.0 (12), 72.0 (100). $C_{13}H_{12}BrNOS$ (310.21): calcd. C 50.33, H 3.90, N 4.52; found C 50.08, H 3.83, N 4.32.

6-Bromonaphthalene-2-thiol (14): A solution of the **13** (3.48 g, 11.2 mmol) in MeOH (250 mL) was saturated with Ar. Then solid KOH (5.22 g, 93.0 mmol) was added and it was heated to 80 °C for 2.5 h. The reaction mixture was then quenched with 1 M aqueous HCl (250 mL) at 0 °C and it was extracted with CH_2Cl_2 (300 mL). The aqueous phase was washed with CH_2Cl_2 (2 × 100 mL). The combined organic phases were washed with brine, dried with $MgSO_4$ and evaporated to give the thiol **14** as a beige solid (2.60 g, 10.9 mmol, 97%); m.p. 175.6–178.6 °C. TLC R_f = 0.21 (hexane/EtOAc = 5:1). ^{1}H NMR (400 MHz, $CDCl_3$, 25 °C): δ = 7.92 (s, 1 H), 7.69 (s, 1 H), 7.61 (d, $^3J_{H,H}$ = 8.6 Hz, 1 H), 7.55 (d, $^3J_{H,H}$ = 8.8 Hz, 1 H), 7.52 (dd, $^2J_{H,H}$ = 1.8, $^3J_{H,H}$ = 8.8 Hz, 1 H), 7.34 (dd, $^2J_{H,H}$ = 1.9, $^3J_{H,H}$ = 8.6 Hz, 1 H), 3.60 (s, 1 H, SH) ppm. ^{13}C NMR (101 MHz, $CDCl_3$, 25 °C): δ = 132.8, 132.6, 130.5, 130.2, 129.5, 129.2, 128.8, 128.1, 127.3, 119.8 ppm. MS (EI): *m*/*z* (%) = 239.9 (100) 237.9 (98) [M$^+$]. $C_{10}H_7BrS$ (239.13): calcd. C 50.23, H 2.95; found C 50.14, H 2.96.

6-Bromonaphthalene-2-[2-(trimethylsilyl)ethyl]thiol (15): The thiol **14** (2.05 g, 8.57 mmol), vinyl-trimethylsilane (5.5 mL, 37.9 mmol) and 2,2′-azobis(2-methylpropionitrile) (AIBN) (70.0 mg, 0.426 mmol) were placed in a 25 mL pressure tube. The tube was sealed and it was stirred for 24 h at 100 °C. The reaction mixture was then evaporated. A precipitate was formed which was filtered off and washed with chloroform. The filtrate was evaporated and dried at high vacuum to give compound **15** as a beige solid (2.78 g, 8.19 mmol, 96%); m.p. 39.3–40.3 °C. TLC R_f = 0.29 (hexane/CH_2Cl_2 = 10:1). ^{1}H NMR (400 MHz, $CDCl_3$, 25 °C): δ = 7.94 (d, $^2J_{H,H}$ = 1.7 Hz, 1 H), 7.65 (m, 2 H), 7.61 (d, $^3J_{H,H}$ = 8.8 Hz, 1 H), 7.53 (dd, $^2J_{H,H}$ = 1.9, $^3J_{H,H}$ = 8.7 Hz, 1 H), 7.41 (dd, $^2J_{H,H}$ = 1.9, $^3J_{H,H}$ = 8.6 Hz, 1 H), 3.06 (m, 2 H, CH_2), 0.55 (m, 2 H, CH_2), 0.07 (s, 9 H, $SiMe_3$) ppm. ^{13}C NMR (101 MHz, $CDCl_3$, 25 °C): δ = 135.7, 132.5, 132.2, 129.82, 129.75, 128.6, 128.0, 127.3, 125.7, 119.1, 29.1, 16.7, –1.7 ppm. MS (EI): *m*/*z* (%) = 340.0 (11) 338.0 (11) [M$^+$], 73.0 (100). $C_{15}H_{19}BrSSi$ (339.37): calcd. C 53.09, H 5.64; found C 53.23, H 5.65.

6-[2-(Trimethylsilyl)ethylthio]naphthalen-2-ylboronic Acid (16): Bromide **15** (1.12 g, 3.29 mmol) was dissolved in THF (15 mL) in a 25 mL Schlenk flask. *n*BuLi (1.6 M in hexane, 3.50 mL, 5.60 mmol) was added at –78 °C and it was stirred for 25 min at this temperature. Then triisopropyl borate (3.50 mL, 15.2 mmol) was added. The reaction mixture was stirred for 1.7 h at –78 °C, 2 h at –20 °C and 3 h at room temperature. The reaction mixture was then quenched with water and extracted with TBME. The aqueous phase was washed with TBME (3 × 50 mL). The combined organic phases were washed with brine (2 × 50 mL), dried with $MgSO_4$ and the solvents evaporated. The crude was recrystallized from hexane to give boronic acid **16** as a beige solid (757 mg, 2.49 mmol, 76%); m.p. 169.8–172.7 °C. ^{1}H NMR (400 MHz, $CDCl_3$, 25 °C): δ = 8.72 (s, 1 H), 8.24 (d, $^3J_{H,H}$ = 8.2 Hz, 1 H), 7.93 (d, $^3J_{H,H}$ = 8.6 Hz, 1 H), 7.83 (d, $^3J_{H,H}$ = 8.2 Hz, 1 H), 7.67 (s, 1 H), 7.43 (d, $^3J_{H,H}$ = 8.6 Hz, 1 H), 3.11 (m, 2 H, CH_2), 1.04 (m, 2 H, CH_2), 0.11 (s, 9 H, $SiMe_3$) ppm. ^{13}C NMR (101 MHz, $CDCl_3$, 25 °C): δ = 137.2, 137.5, 136.2, 131.4, 130.8, 129.3, 126.6, 126.3, 124.8, 28.7, 16.6, –1.7 ppm. MS (MALDI-TOF): found *m*/*z* = 299.13, 304.11 calculated for $C_{15}H_{21}BO_2SSi$.

1,4-Bis{6-[2-(trimethylsilyl)ethylthio]naphthalen-2-yl}-2,5-bis[(*E*)-pyridin-4-ylvinyl]benzene (17): Iodide **5** (87 mg, 0.162 mmol) and boronic acid **16** (110 mg, 0.362 mmol) were suspended in toluene (8 mL) and ethanol (2 mL). The mixture was degassed, before $Pd(PPh_3)_4$ (20 mg, 0.017 mmol) and K_2CO_3 (185 mg, 1.34 mmol) were added. The reaction mixture was exposed to microwaves (500 W, 80 °C) for 140 min. The solid material was filtered off, the filtrate was evaporated and chromatographed (silica gel, 2 × 12 cm, CH_2Cl_2, 1% MeOH to 2% MeOH) to give the cruciform structure **17** as a yellow solid (110 mg, 0.137 mmol, 85%); m.p. 221.0–223.0 °C. TLC R_f = 0.13 (CH_2Cl_2, 2% MeOH). ^{1}H NMR (400 MHz, $CDCl_3$, 25 °C): δ = 8.49 (d, $^3J_{H,H}$ = 6.1 Hz, 4 H), 7.90–7.87 (m, 6 H), 7.83 (d, $^3J_{H,H}$ = 8.7 Hz, 2 H), 7.79 (s, 2 H), 7.59 (dd, $^2J_{H,H}$ = 1.7, $^3J_{H,H}$ = 8.4 Hz, 2 H), 7.49 (dd, $^2J_{H,H}$ = 1.8, $^3J_{H,H}$ = 8.6 Hz, 2 H), 7.40 (d, $^3J_{H,H}$ = 16.3 Hz, 2 H), 7.18 (d, $^3J_{H,H}$ = 6.2 Hz, 4 H), 7.07 (d, $^3J_{H,H}$ = 16.2 Hz, 2 H), 3.13 (m, 4 H, CH_2), 1.04 (m, 4 H, CH_2), 0.10 (s, 18 H, $SiMe_3$) ppm. ^{13}C NMR (101 MHz, $CDCl_3$, 25 °C): δ = 150.2, 144.4, 141.1, 136.9, 136.0, 134.6, 133.0, 131.4, 131.3, 128.53, 128.52, 128.4, 128.3, 127.8, 127.5, 127.0, 125.6, 120.8, 29.2, 16.8, –1.7 ppm. MS (EI): *m*/*z* (%) = 801.2 (21) 800.3 (32) [M$^+$], 772.3 (24) 73.0 (100). UV: λ_{max} = 325 nm. GPC (oligopore 6 μm, toluene, UV/Vis photodiode array detector) area 99.1%.

1,4-Bis(6-thioacetylnaphthalen-2-yl)-2,5-bis[(*E*)-pyridin-4-ylvinyl]-benzene (4): The ethyl-TMS-protected thiol **17** (190 mg, 0.237 mmol) was dissolved in THF (25 mL) in a 100 mL flask. The mixture was degassed before TBAF (1 M in THF, 4.00 mL, 4.00 mmol) was added. It was stirred for 1 h, then acetyl chloride (0.600 mL, 8.45 mmol) was added and it was stirred for 30 min. The reaction mixture was quenched with ethanol (25 mL) and chloroform (25 mL). After stirring for 15 min, the reaction mixture was extracted with water (200 mL) and CH_2Cl_2 (100 mL). The aqueous phase was washed with CH_2Cl_2 (3 × 50 mL). The combined organic phases were washed with brine, dried with $MgSO_4$ and the solvents evaporated. The crude was purified by column chromatography (silica gel, 2 × 12 cm, CH_2Cl_2, 1% MeOH to 2% MeOH) to give the acetylated cruciform **3** as a yellowish solid (94.0 mg, 0.137 mmol, 58%). TLC R_f = 0.25 (CH_2Cl_2, 5% MeOH); m.p. (decomp.) above 250 °C. ^{1}H NMR (400 MHz, $CDCl_3$, 25 °C): δ = 8.49 (d, $^3J_{H,H}$ = 5.9 Hz, 4 H), 8.06 (s, 2 H), 7.98–7.95 (m, 6 H), 7.89 (s, 2 H), 7.63 (dd, $^2J_{H,H}$ = 1.6, $^3J_{H,H}$ = 8.5 Hz, 2 H), 7.55 (dd, $^2J_{H,H}$ = 1.7, $^3J_{H,H}$ = 8.5 Hz, 2 H), 7.38 (d, $^3J_{H,H}$ = 16.3 Hz, 2 H), 7.21 (d, $^3J_{H,H}$ = 6.2 Hz, 4 H), 7.09 (d, $^3J_{H,H}$ = 16.2 Hz, 2 H), 2.51 (s, 6 H, CH_3) ppm. ^{13}C NMR (101 MHz, $CDCl_3$, 25 °C): δ = 194.2, 150.2, 144.3, 141.0, 138.7, 134.6, 134.3, 133.3, 132.8, 131.8, 130.9, 129.0, 128.6, 125.5, 128.3, 128.1, 127.8, 126.0, 120.9, 30.4 ppm. MS (MALDI-TOF): found *m*/*z* = 684.07, 684.19 calculated for $C_{44}H_{32}N_2O_2S_2$. UV/Vis: λ_{max} = 316 nm. GPC (oligopore 6 μm, toluene, UV/Vis photodiode array detector) area 99.1%.

2,5-Bis{6-[2-(trimethylsilyl)ethylthio]naphthalen-2-yl}-*p*-xylene (21): 2,5-Diiodo-*p*-xylene (91.0 mg, 0.254 mmol) and boronic acid **16** (170 mg, 0.557 mmol) were dissolved in toluene (6 mL) and ethanol (1.5 mL). The mixture was argon-saturated before $Pd(PPh_3)_4$ (66 mg, 0.057 mmol) and K_2CO_3 (285 mg, 2.06 mmol) was added. The reaction mixture was then stirred for 15 h at 80 °C. The insoluble material was filtered off and washed with toluene. The filtrate was evaporated and purified by column chromatography (silica gel,

3×12 cm, CH_2Cl_2/hexane = 1:1) to give **21** as a colourless solid (158.3 mg, 0.254 mmol, 100%); m.p. 138.0–141.0 °C. TLC R_f = 0.49 (CH_2Cl_2/hexane = 1:1). ^{1}H NMR (400 MHz, $CDCl_3$, 25 °C): δ = 7.82–7.77 (m, 8 H), 7.54 (d, $^3J_{H,H}$ = 8.4 Hz, 2 H), 7.46 (d, $^3J_{H,H}$ = 8.6 Hz, 2 H), 7.28 (s, 2 H), 3.10 (m, 4 H, CH_2), 2.35 (s, 6 H, Me), 1.01 (m, 4 H, CH_2), 0.08 (s, 18 H, $SiMe_3$) ppm. ^{13}C NMR (101 MHz, $CDCl_3$, 25 °C): δ = 140.7, 138.9, 134.8, 132.9, 132.6, 132.1, 131.5, 128.4, 127.66, 127.65, 126.6, 126.3, 29.5, 20.0, 16.9, –1.7 ppm. MS (EI): *m*/*z* (%) = 623.3 (26), 622.3 (49) [M$^+$], 566.2 (37), 73.1 (100).

2,5-Bis(6-thioacetylnaphthalen-2-yl)-*p*-xylene (22): The starting material **21** (104 mg, 0.167 mmol) was dissolved in THF (8 mL). The solution was degassed, before TBAF (1 M in THF, 1.70 mL, 1.70 mmol) was added. After stirring for 45 min at room temperature more TBAF was added (1 M in THF, 1.00 mL, 1.00 mmol). It was stirred for 2 h, then more TBAF (1 M in THF, 0.60 mL, 0.60 mmol) was added and it was stirred for another 30 min. Then acetyl chloride (0.5 mL, 7.04 mmol) was added dropwise. The reaction mixture was poured onto ice and extracted with CH_2Cl_2. The aqueous phase was washed with CH_2Cl_2 (2×50 mL). The combined organic phase was washed with brine, dried with $MgSO_4$ and the solvents evaporated. The crude was purified by column chromatography (silica gel, 2×12 cm, CH_2Cl_2/hexane = 1:1) to give the acetylated rod **22** as a colourless solid (39.0 mg, 0.0770 mmol, 46%); m.p. 197.6–200.2 °C. TLC R_f = 0.55 (CH_2Cl_2). ^{1}H NMR (400 MHz, $CDCl_3$, 25 °C): δ = 8.01 (s, 2 H), 7.93–7.89 (m, 4 H), 7.87 (s, 2 H), 7.59 (dd, $^2J_{H,H}$ = 1.4, $^3J_{H,H}$ = 8.4 Hz, 2 H), 7.51 (dd, $^2J_{H,H}$ = 1.5, $^3J_{H,H}$ = 8.5 Hz, 2 H), 7.29 (s, 2 H), 2.49 (s, 6 H, CH_3), 2.34 (s, 6 H, Me) ppm. ^{13}C NMR (101 MHz, $CDCl_3$, 25 °C): δ = 194.4, 140.7, 140.6, 134.2, 133.3, 132.9, 132.4, 132.1, 131.3, 128.9, 128.5, 127.7, 121.7, 125.2, 30.3, 20.0 ppm. MS (EI): *m*/*z* (%) = 506.1 (31) [M$^+$], 464.1 (35), 422.2 (100). UV/Vis: λ_{max} 231, 261, 301 nm. GPC (oligopore 6 µm, toluene, UV/Vis photodiode array detector) area 99.0%.

1,4-Bis{4-[2-(trimethylsilyl)ethylthio]phenyl}-2,5-bis[(*E*)-2-phenylethenyl]benzene (24): Iodide **23** (116 mg, 0.217 mmol) and boronic acid **8** (121 mg, 0.476 mmol) were dissolved in toluene (8 mL) and ethanol (2 mL). The mixture was degassed, before $Pd(PPh_3)_4$ (20 mg, 0.0173 mmol) and K_2CO_3 (239 mg, 1.74 mmol) were added. The reaction mixture was exposed to microwaves (500 W, 85 °C) for 4 h. The reaction mixture was then evaporated, absorbed on silica and chromatographed (silica gel, 2×12 cm, CH_2Cl_2/hexane = 1:4 to 1:2) to give **24** as a colourless solid (110 mg, 0.157 mmol, 73%). TLC R_f = 0.61 (CH_2Cl_2/hexane = 1:1). ^{1}H NMR (400 MHz, $CDCl_3$, 25 °C): δ = 7.42 (m, 12 H), 7.31 (t, $^3J_{H,H}$ = 7.5 Hz, 4 H), 7.23 (t, $^3J_{H,H}$ = 7.2 Hz, 2 H), 7.16 (d, $^3J_{H,H}$ = 16.3 Hz, 2 H), 7.08 (d, $^3J_{H,H}$ = 16.2 Hz, 2 H), 3.06 (m, 4 H, CH_2), 1.02 (m, 4 H, CH_2), 0.09 (s, 18 H, $SiMe_3$) ppm. ^{13}C NMR (101 MHz, $CDCl_3$, 25 °C): δ = 139.8, 137.7, 137.4, 136.7, 134.6, 130.3, 129.7, 128.7, 128.2, 127.62, 127.57, 127.0, 126.6, 29.3, 16.9, –1.7 ppm. MS (EI): *m*/*z* (%) = 698.3 (95) [M$^+$], 73.0 (100).

1,4-Bis(4-thioacetylphenyl)-2,5-bis[(*E*)-2-phenylethenyl]benzene (25): Compound **24** (92.0 mg, 0.132 mmol) was dissolved in THF (10 mL). The mixture was degassed, before TBAF (1 M in THF, 3.00 mL, 3.00 mmol) was added. After stirring for 55 min at room temperature, acetyl chloride (0.500 mL, 7.04 mmol) was added at 0 °C. The reaction mixture was stirred for 40 min at room temp. and then quenched with water at 0 °C. The mixture was then extracted with CH_2Cl_2. The aqueous phase was washed with CH_2Cl_2. The combined organic phase was dried with $MgSO_4$, evaporated and chromatographed (silica gel, 2×12 cm, CH_2Cl_2/hexane = 1:1) to give the cruciform **25** as a colourless solid (28.0 mg, 0.0480 mmol, 36%). TLC R_f = 0.41 (CH_2Cl_2/hexane = 1:1); m.p. 237–239 °C followed by decomp. ^{1}H NMR (400 MHz, $CDCl_3$, 25 °C): δ = 7.76 (s, 2 H), 7.55 (s, 8 H), 7.40 (d, $^3J_{H,H}$ = 7.3 Hz, 4 H), 7.32 (t, $^3J_{H,H}$ = 7.5 Hz, 4 H), 7.24 (t, $^3J_{H,H}$ = 7.2 Hz, 2 H), 7.12 (m, 4 H), 2.49 (s, 6 H, CH_3) ppm. ^{13}C NMR (101 MHz, $CDCl_3$, 25 °C): δ = 194.0, 141.6, 139.7, 137.2, 134.7, 134.2, 130.7, 130.3, 128.7, 127.8, 127.7, 127.0, 126.6, 126.4, 30.3 ppm. MS (EI): *m*/*z* (%) = 582.2 (100) [M$^+$], 540.2 (96), 498.1 (38). UV/Vis: λ_{max} = 295, 347 nm. GPC (oligopore 6 µm, toluene, UV/Vis photodiode array detector) area 99.2%.

1,4-Bis{6-[2-(trimethylsilyl)ethylthio]naphthalen-2-yl}-2,5-bis[(*E*)-2-phenylethenyl]benzene (26): Iodide **23** (91.0 mg, 0.170 mmol) and boronic acid **16** (107 mg, 0.352 mmol) were dissolved in toluene (8 mL) and ethanol (2 mL). The mixture was degassed, before $Pd(PPh_3)_4$ (25 mg, 0.0217 mmol) and K_2CO_3 (188 mg, 1.36 mmol) were added. The reaction mixture was exposed to microwaves (500 W, 85 °C) for 3 h and then evaporated, absorbed on silica gel and chromatographed (silica gel, 2×12 cm, hexane/CH_2Cl_2 = 5:1 to 1:1) to give **26** as a colourless solid (73.0 mg, 0.0913 mmol, 54%). TLC R_f = 0.60 (CH_2Cl_2/hexane = 1:1). ^{1}H NMR (400 MHz, $CDCl_3$, 25 °C): δ = 7.94 (s, 2 H), 7.87–7.83 (m, 6 H), 7.80 (s, 2 H), 7.64 (dd, $^2J_{H,H}$ = 1.7, $^3J_{H,H}$ = 8.4 Hz, 2 H), 7.48 (dd, $^2J_{H,H}$ = 1.8, $^3J_{H,H}$ = 8.5 Hz, 2 H), 7.35 (d, $^3J_{H,H}$ = 7.2 Hz, 4 H), 7.27 (t, $^3J_{H,H}$ = 7.4 Hz, 4 H), 7.24–7.20 (m, 4 H), 7.15 (d, $^3J_{H,H}$ = 16.2 Hz, 2 H), 3.13 (m, 4 H, CH_2), 1.04 (m, 4 H, CH_2), 0.10 (s, 18 H, $SiMe_3$) ppm. ^{13}C NMR (101 MHz, $CDCl_3$, 25 °C): δ = 140.4, 137.7, 137.4, 135.4, 134.8, 132.9, 131.5, 129.8, 128.9, 128.6, 128.5, 128.4, 127.8, 127.7, 127.6, 127.0, 126.8, 126.6, 125.9, 29.3, 16.8, –1.7 ppm. MS (EI): *m*/*z* (%) = 798.3 (100) [M$^+$].

1,4-Bis(6-thioacetylnaphthalen-2-yl)-2,5-bis[(*E*)-2-phenylethenyl]-benzene (27): The ethyl-TMS-protected cruciform **26** (55 mg, 0.070 mmol) was dissolved in 10 mL of THF. It was degassed for 10 min before TBAF (1 M in THF, 2.00 mL, 2.00 mmol) was added at room temperature. The reaction mixture was stirred for 55 min, then acetyl chloride (0.40 mL, 4.61 mmol) was added at 0 °C. The mixture was stirred for 40 min. Then 5 mL of ethanol was added and it was extracted with water and DCM. The aqueous phase was washed twice with DCM. The combined organic phases were washed with water, dried with $MgSO_4$, evaporated and purified by column chromatography (silica, 2×12 cm, CH_2Cl_2/hexane = 1:3 to 1:1) to give the product **27** as a colourless solid (9.00 mg, 0.0132 mmol, 19%). TLC R_f = 0.37 (CH_2Cl_2/hexane = 1:1); m.p. 301–304 °C. ^{1}H NMR (400 MHz, $CDCl_3$, 25 °C): δ = 8.05 (s, 2 H), 8.01 (s, 2 H), 7.96 (m, 4 H), 7.86 (s, 2 H), 7.68 (dd, $^2J_{H,H}$ = 1.7, $^3J_{H,H}$ = 8.5 Hz, 2 H), 7.53 (dd, $^2J_{H,H}$ = 1.7, $^3J_{H,H}$ = 8.5 Hz, 2 H), 7.35 (d, $^3J_{H,H}$ = 7.2 Hz, 4 H), 7.28 (m, 4 H), 7.21 (m, 2 H), 7.17 (s, 4 H), 2.51 (s, 6 H, CH_3) ppm. ^{13}C NMR (126 MHz, $CDCl_3$, 25 °C): δ = 194.3, 140.3, 139.5, 137.3, 134.8, 134.3, 133.3, 132.7, 131.5, 130.1, 129.1, 129.0, 128.7, 128.5, 127.9, 127.7, 126.6 (6 C), 125.6 ppm. MS (EI): *m*/*z* (%) = 682.2 (7) [M$^+$], 640.2 (41), 598.2 (100). UV/Vis: λ_{max} 317, 354 nm. GPC (oligopore 6 µm, toluene, UV/Vis photodiode array detector) area 99.6%.

Supporting Information (see also the footnote on the first page of this article): The synthesis of compound **11** as well as the ^{1}H NMR and ^{13}C NMR spectra for compounds **3**, **4**, **8**, **9**, **11**–**22**, **24**–**27** are given.

Acknowledgments

Financial support by the Swiss National Science Foundation (SNSF), the National Center of Competence in Research "Nano-

scale Science" and the Gebert Rüf Foundation is gratefully acknowledged.

[1] H. Kuhn, *Struct. Chem. Mol. Biol.* **1968**, 566.
[2] A. Aviram, M. A. Ratner, *Chem. Phys. Lett.* **1974**, *29*, 277.
[3] R. M. Metzger, *Acc. Chem. Res.* **1999**, *32*, 950.
[4] M.-K. Ng, L. Yu, *Angew. Chem. Int. Ed.* **2002**, *41*, 3598.
[5] J. G. Kushmerick, D. B. Holt, J. C. Yang, J. Naciri, M. H. Moore, R. Shashidhar, *Phys. Rev. Lett.* **2002**, *89*, 086802.
[6] R. E. Holmlin, R. F. Ismagilov, R. Haag, V. Mujica, M. A. Ratner, M. A. Rampi, G. M. Whitesides, *Angew. Chem. Int. Ed.* **2001**, *40*, 2316.
[7] J. M. Mativetsky, G. Pace, M. Elbing, M. A. Rampi, M. Mayor, P. Samorí, *J. Am. Chem. Soc.* **2008**, *130*, 9192.
[8] G. Pace, V. Ferri, C. Grave, M. Elbing, C. von Hänisch, M. Zharnikov, M. Mayor, M. A. Rampi, P. Samorí, *Proc. Natl. Acad. Sci. USA* **2007**, *104*, 9937.
[9] J. Chen, M. A. Reed, A. M. Rawlett, J. M. Tour, *Science (Washington DC)* **1999**, *286*, 1550.
[10] A. Wassel Ronald, B. Gorman Christopher, *Angew. Chem. Int. Ed.* **2004**, *43*, 5120.
[11] M. Mayor, H. B. Weber, *Chimia* **2003**, *56*, 494.
[12] C. Joachim, J. K. Gimzewski, A. Aviram, *Nature* **2000**, *408*, 541.
[13] N. J. Tao, *Nat. Nanotechnol.* **2006**, *1*, 173.
[14] N. Weibel, S. Grunder, M. Mayor, *Org. Biomol. Chem.* **2007**, *5*, 2343.
[15] L. A. Bumm, J. J. Arnold, M. T. Cygan, T. D. Dunbar, T. P. Burgin, L. Jones II, D. L. Allara, J. M. Tour, P. S. Weiss, *Science (Washington DC)* **1996**, *271*, 1705.
[16] X. D. Cui, A. Primak, X. Zarate, J. Tomfohr, O. F. Sankey, A. L. Moore, T. A. Moore, D. Gust, G. Harris, S. M. Lindsay, *Science (Washington DC)* **2001**, *294*, 571.
[17] B. Xu, N. J. Tao, *Science (Washington DC)* **2003**, *301*, 1221.
[18] L. Venkataraman, J. E. Klare, I. W. Tam, C. Nuckolls, M. S. Hybertsen, M. L. Steigerwald, *Nano Lett.* **2006**, *6*, 458.
[19] L. Grüter, M. T. González, R. Huber, M. Calame, C. Schönenberger, *Small* **2005**, *1*, 1067.
[20] J. Reichert, R. Ochs, D. Beckmann, H. B. Weber, M. Mayor, H. von Lohneysen, *Phys. Rev. Lett.* **2002**, *88*, 176804/1.
[21] M. A. Reed, C. Zhou, C. J. Muller, T. P. Burgin, J. M. Tour, *Science (Washington DC)* **1997**, *278*, 252.
[22] C. Kergueris, J. P. Bourgoin, S. Palacin, D. Esteve, C. Urbina, M. Magoga, C. Joachim, *Phys. Rev. B* **1999**, *59*, 12505.
[23] R. H. M. Smit, Y. Noat, C. Untiedt, N. D. Lang, M. C. van Hemert, J. M. van Ruitenbeek, *Nature* **2002**, *419*, 906.
[24] C. A. Martin, D. Ding, J. K. Sørensen, T. Bjørnholm, J. M. van Ruitenbeek, H. S. J. van der Zant, *J. Am. Chem. Soc.* **2008**, *130*, 13198.
[25] J. Park, A. N. Pasupathy, J. I. Goldsmith, C. Chang, Y. Yaish, J. R. Petta, M. Rinkoski, J. P. Sethna, H. D. Abruna, P. L. McEuen, D. C. Ralph, *Nature* **2002**, *417*, 722.
[26] Z. M. Wu, M. Steinacher, R. Huber, M. Calame, S. J. van der Molen, C. Schönenberger, *Appl. Phys. Lett.* **2007**, *91*, 053118/1.
[27] E. A. Osorio, K. O'Neill, M. Wegewijs, N. Stuhr-Hansen, J. Paaske, T. Bjørnholm, H. S. J. van der Zant, *Nano Lett.* **2007**, *7*, 3336.
[28] F. Chen, X. Li, J. Hihath, Z. Huang, N. Tao, *J. Am. Chem. Soc.* **2006**, *128*, 15874.
[29] X. Li, J. He, J. Hihath, B. Xu, S. M. Lindsay, N. Tao, *J. Am. Chem. Soc.* **2006**, *128*, 2135.
[30] W. Wang, T. Lee, M. A. Reed, *Phys. Rev. B* **2003**, *68*, 035416.
[31] W. Wang, T. Lee, M. A. Reed, *J. Phys. Chem. B* **2004**, *108*, 18398.
[32] M. T. González, S. Wu, R. Huber, S. J. van der Molen, C. Schönenberger, M. Calame, *Nano Lett.* **2006**, *6*, 2238.
[33] R. Huber, M. T. González, S. Wu, M. Langer, S. Grunder, V. Horhoiu, M. Mayor, M. R. Bryce, C. Wang, R. Jitchati, C. Schönenberger, M. Calame, *J. Am. Chem. Soc.* **2008**, *130*, 1080.
[34] D. S. Seferos, S. A. Trammell, G. C. Bazan, J. G. Kushmerick, *Proc. Natl. Acad. Sci. USA* **2005**, *102*, 8821.
[35] J. G. Kushmerick, D. B. Holt, S. K. Pollack, M. A. Ratner, J. C. Yang, T. L. Schull, J. Naciri, M. H. Moore, R. Shashidhar, *J. Am. Chem. Soc.* **2002**, *124*, 10654.
[36] L. T. Cai, H. Skulason, J. G. Kushmerick, S. K. Pollack, J. Naciri, R. Shashidhar, D. L. Allara, T. E. Mallouk, T. S. Mayer, *J. Phys. Chem. B* **2004**, *108*, 2827.
[37] J. Liao, M. A. Mangold, S. Grunder, M. Mayor, C. Schönenberger, M. Calame, *New J. Phys.* **2008**, *10*, 065019.
[38] E. Lörtscher, M. Elbing, M. Tschudy, C. von Hänisch, H. B. Weber, M. Mayor, H. Riel, *ChemPhysChem* **2008**, *9*, 2252.
[39] J. G. Kushmerick, C. M. Whitaker, S. K. Pollack, T. L. Schull, R. Shashidhar, *Nanotechnology* **2004**, *15*, S489.
[40] M. Elbing, R. Ochs, M. Koentopp, M. Fischer, C. von Hänisch, F. Weigend, F. Evers, H. Weber, M. Mayor, *Proc. Natl. Acad. Sci. USA* **2005**, *102*, 8815.
[41] D. Dulic, S. J. van der Molen, T. Kudernac, H. T. Jonkman, J. J. D. de Jong, T. N. Bowden, J. van Esch, B. L. Feringa, B. J. van Wees, *Phys. Rev. Lett.* **2003**, *91*, 207402/1.
[42] D. I. Gittins, D. Bethell, D. J. Schiffrin, R. J. Nichols, *Nature* **2000**, *408*, 67.
[43] W. Haiss, H. Van Zalinge, S. J. Higgins, D. Bethell, H. Hoebenreich, D. J. Schiffrin, R. J. Nichols, *J. Am. Chem. Soc.* **2003**, *125*, 15294.
[44] Z. Li, B. Han, G. Meszaros, I. Pobelov, T. Wandlowski, A. Błaszczyk, M. Mayor, *J. Chem. Soc. Faraday Trans.* **2006**, *131*, 121.
[45] B. Han, Z. Li, T. Wandlowski, A. Błaszczyk, M. Mayor, *J. Phys. Chem. C* **2007**, *111*, 13855.
[46] Z. Li, I. Pobelov, B. Han, T. Wandlowski, A. Błaszczyk, M. Mayor, *Nanotechnology* **2007**, *18*, 044018/1.
[47] X. Xiao, D. Brune, J. He, S. Lindsay, C. B. Gorman, N. Tao, *Chem. Phys.* **2006**, *326*, 138.
[48] F. Chen, N. J. Tao, *Acc. Chem. Res.* **2009**, *42*, 429.
[49] H. Yu, Y. Luo, K. Beverly, J. F. Stoddart, H.-R. Tseng, R. Heath James, *Angew. Chem. Int. Ed.* **2003**, *42*, 5706.
[50] E. Lörtscher, J. W. Ciszek, J. Tour, H. Riel, *Small* **2006**, *2*, 973.
[51] V. Ferri, M. Elbing, G. Pace, M. D. Dickey, M. Zharnikov, P. Samorì, M. Mayor, M. A. Rampi, *Angew. Chem. Int. Ed.* **2008**, *47*, 3407.
[52] M. Elbing, A. Błaszczyk, C. von Hänisch, M. Mayor, V. Ferri, C. Grave, M. A. Rampi, G. Pace, P. Samorì, A. Shaporenko, M. Zharnikov, *Adv. Funct. Mater.* **2008**, *18*, 2972.
[53] S. Grunder, R. Huber, V. Horhoiu, M. T. González, C. Schönenberger, M. Calame, M. Mayor, *J. Org. Chem.* **2007**, *72*, 8337.
[54] A. Błaszczyk, M. Fischer, C. von Hänisch, M. Mayor, *Eur. J. Org. Chem.* **2007**, 2630.
[55] A. Błaszczyk, M. Chadim, C. von Hänisch, M. Mayor, *Eur. J. Org. Chem.* **2006**, 3809.
[56] N. Weibel, A. Mishchenko, T. Wandlowski, M. Neuburger, Y. Leroux, M. Mayor, *Eur. J. Org. Chem.* **2009**, 6140.
[57] X. Li, J. Hihath, F. Chen, T. Masuda, L. Zang, N. J. Tao, *J. Am. Chem. Soc.* **2007**, *129*, 11535.
[58] D. Mayer, T. Dretschkow, K. Ataka, T. Wandlowski, *J. Electroanal. Chem.* **2002**, *524–525*, 20.
[59] T. Wandlowski, K. Ataka, D. Mayer, *Langmuir* **2002**, *18*, 4331.
[60] B. Q. Xu, X. L. Li, X. Y. Xiao, H. Sakaguchi, N. J. Tao, *Nano Lett.* **2005**, *5*, 1491.
[61] J. E. Klare, G. S. Tulevski, K. Sugo, A. de Picciotto, K. A. White, C. Nuckolls, *J. Am. Chem. Soc.* **2003**, *125*, 6030.
[62] H. Kang, P. Zhu, Y. Yang, A. Facchetti, T. J. Marks, *J. Am. Chem. Soc.* **2004**, *126*, 15974.
[63] H. Kang, G. Evmenenko, P. Dutta, K. Clays, K. Song, T. J. Marks, *J. Am. Chem. Soc.* **2006**, *128*, 6194.
[64] J. N. Wilson, M. Josowicz, Y. Wang, U. H. F. Bunz, *Chem. Commun.* **2003**, 2962.
[65] J. N. Wilson, U. H. F. Bunz, *J. Am. Chem. Soc.* **2005**, *127*, 4124.

[66] M. Hauck, J. Schoenhaber, A. J. Zucchero, K. I. Hardcastle, T. J. J. Mueller, U. H. F. Bunz, *J. Org. Chem.* **2007**, *72*, 6714.
[67] J. Tolosa, A. J. Zucchero, U. H. F. Bunz, *J. Am. Chem. Soc.* **2008**, *130*, 6498.
[68] P. L. McGrier, K. M. Solntsev, J. Schoenhaber, S. M. Brombosz, L. M. Tolbert, U. H. F. Bunz, *Chem. Commun.* **2007**, 2127.
[69] A. J. Zucchero, J. N. Wilson, U. H. F. Bunz, *J. Am. Chem. Soc.* **2006**, *128*, 11872.
[70] W. W. Gerhardt, A. J. Zucchero, J. N. Wilson, C. R. South, U. H. F. Bunz, M. Weck, *Chem. Commun.* **2006**, 2141.
[71] M. Mayor, B. Weber Heiko, J. Reichert, M. Elbing, C. Von Hänisch, D. Beckmann, M. Fischer, *Angew. Chem. Int. Ed.* **2003**, *42*, 5834.
[72] C. J. Yu, Y. Chong, J. F. Kayyem, M. Gozin, *J. Org. Chem.* **1999**, *64*, 2070.
[73] J. N. Wilson, P. M. Windscheif, U. Evans, M. L. Myrick, U. H. F. Bunz, *Macromolecules* **2002**, *35*, 8681.
[74] K. Freudenberg, D. Peters, *Ber. Dtsch. Chem. Ges. [Abteilung] B: Abhandlungen* **1919**, *52*, 1463.
[75] M. S. Newman, H. A. Karnes, *J. Org. Chem.* **1966**, *31*, 3980.
[76] H. Kwart, E. R. Evans, *J. Org. Chem.* **1966**, *31*, 410.
[77] G. C. Lloyd-Jones, J. D. Moseley, J. S. Renny, *Synthesis* **2008**, 661.
[78] F. Beaulieu, V. Snieckus, *Synthesis* **1992**, 112.
[79] H. Detert, O. Sadovski, E. Sugiono, *J. Phys. Org. Chem.* **2004**, *17*, 1046.
[80] Note that, for compound **1**, no molecular signature was observed in such experiments. This probably stems from the fact that this cross has a conductance located below the detection limit of the setup due to the *meta* position of the anchor groups. Compound **2** provided a clear signal with a well-defined single peak in the log(*G*) histogram (see ref.[53]).
[81] A. Brikh, C. Morin, *J. Organomet. Chem.* **1999**, *581*, 82.

Received: October 12, 2009
Published Online: January 4, 2010

